

Data-driven Estimation of Background Distribution through Neural Autoregressive Flows

Suyong Choi, Jaehoon Lim, Hayoung Oh

Korea University, Department of Physics, Seoul 02841, Republic of Korea

E-mail: suyong@korea.ac.kr, chaosbringer@korea.ac.kr,
alice0102@korea.ac.kr

ABSTRACT: We report on a general and automatic data-driven background distribution shape estimation method using neural autoregressive flows (NAF), which is one of the deep generative learning methods. Data-driven background estimation is indispensable for many analyses involving complicated final states where reliable predictions are not available. NAF allow us to construct general bijective transformations that operate on multidimensional space, out of finite number of invertible one-dimensional functions. Given its simplicity and universality, it is well suited to the application in the data-driven background estimation, since data-driven estimations can be expressed as transformations. In a data-driven background estimation, the goal is to derive appropriate transformations and apply extrapolated transformations to the region of interest. In the ABCDnn method, we can have the NAF learn the transformations' dependence on control variables by having multiple control regions. We demonstrate that the prediction through ABCDnn method is similar to optimal case, while having smaller statistical uncertainty.

Contents

1	Introduction	1
2	Data-driven Background Estimation as Transformation	2
3	Neural Autoregressive Flows for Data-driven Shape Estimation	3
3.1	Neural Autoregressive Flows	3
3.2	NAF for shape estimation	4
4	Application of ABCDnn to $t\bar{t} + multijets$	7
5	Conclusions	11

1 Introduction

The LHC experiments have collected about 5% of the total amount expected during their lifetime. However, more data does not necessarily translate to improved sensitivity or precision, as reducing systematic uncertainty is not trivial, one of which is typically due to background estimation. Precise estimations of the backgrounds are becoming increasingly important as rarer processes are being probed. Recent $H \rightarrow \mu^+\mu^-$ results point to the sophistication in background estimation required for optimal signal extraction of a very rare process, once thought to require much more data to probe[1, 2]. With more data, more complicated final states become accessible and will become the focus of the experiments, since it offers new possibilities in probing of new interactions [3]. It is especially for these multiparton final states where the background estimations are difficult.

To obtain a more precise background estimation, we would need combination of higher-order perturbative calculations from theory as well as improved understanding of experimental apparatus and the hadron collision environment, and more advanced analysis techniques. However, for many background processes, next-to leading order perturbative calculations are not available, and even for those that are, the uncertainty is significant compared to experimental uncertainties [4–6]. These may limit the precision of measurements as well as some searches for physics beyond the standard model. While having more statistics will improve some of these limitations, we still need even higher order calculations of many background processes and improved simulations of the experimental apparatus.

The Monte Carlo calculations are essential tools to calculate some of the essential elements of analyses. However, the calculations and simulations must confront the data in a control regions. Differences between the simulation and the real data, in a well-controlled phase space, are used to derive calibrations and corrections to the simulation. Any remaining differences may be a source of experimental systematic uncertainties. Data-driven

techniques are devised to take these differences into account when estimating backgrounds in the region of interest. One way to reduce the systematic uncertainties associated with background estimation is by making use of the large statistics data. Historically, data-driven methods of background estimation, have been essential in bringing about the observations of many new particles [7]-[13].

Despite their wide-spread use and importance, the methods of data-driven background estimation have not been received much scrutiny. We have shown that by extending the existing methods, one could get improvements in predictions compared to the regular ABCD method, by having more control regions [22]. In that study, we derived some formulae for optimal combination of information various control regions for extrapolation or interpolation. We cannot derive these formulae for arbitrary case, however, by incorporating deep learning methods, we could make the optimal use of the information in making background predictions.

In this letter, we introduce a general method of data-driven background shape estimation that is generally applicable, as it can automatically take into consideration the complicated correlations among the feature variables. As a case study, we will apply it to a non-trivial example of $t\bar{t} + multijets$ background estimation.

2 Data-driven Background Estimation as Transformation

In this section, we show that data-driven background estimation can be formulated as a problem in finding transformation to be applied to some base distribution. The problem we consider is that of estimating a distribution of \vec{x} , under certain condition expressed by \vec{c} , which we label as the control variable.

$$p(\vec{x}|\vec{c}) \tag{2.1}$$

The control variable \vec{c} can be used to label different regions of phase space, such as various control regions (CR) and signal regions (SR). We assume that these regions are non-overlapping. A component of \vec{c} could be a real number, if p is to depend on a continuous variable, or it could be an integer if it is used to enumerate different regions of phase space.

The CRs are usually neighbors or next-to-nearest neighbors of the SR multidimensional space spanned by \vec{c} . If the CR completely surrounds the SR then the problem is that of estimating p through interpolation from the distributions in the surrounding CRs. While if signal region cannot be surrounded completely by CRs, then we need to extrapolate out to the SR. The so-called ‘‘ABCD’’ or ‘‘matrix’’ method frequently employed in hadron collider experiments can be used [21] here. Many variations on the idea are possible, from purely data-driven with no dependence on MC, to deriving corrections to MC from the CRs.

To employ these methods, require us to find two independent variables as control variables. With many control regions, such requirements can be relaxed to some degree and analytic expressions for how to make optimal extrapolations are available for some configurations of CR and SR [22]. However, for a general case, we propose to use deep neural networks for data-driven extrapolations, as it should be able learn the non-trivial

correlations among the variables (feature or control variables) and make the most effective use of the information available.

We formalize various data-driven techniques as transformations. Starting from some base distribution $f(\vec{x}; \vec{c})$ and with some transformation \mathcal{T} , we can obtain a new distribution.

$$p'(\vec{x}'|\vec{c}') = \sum_{\vec{c} \neq \vec{c}'} \int \mathcal{T}(\vec{x}'; \vec{x}|\vec{c}'; \vec{c}) p(\vec{x}|\vec{c}) d\vec{x}. \quad (2.2)$$

The transformation would transform from \vec{x} space to \vec{x}' given the condition variable \vec{c} , the condition under which the base distribution is obtained. For simplicity, we will write the convolution operation and summation over \vec{c} as $\mathcal{T} \otimes f$ from now on. All forms of data-driven techniques can be formulated in this manner.

For example, Monte Carlo simulated data distributions are compared to the real data in some background dominated control region \vec{c}_b and then scale factors or calibrations are derived

$$p_{data}(\vec{x}'|\vec{c}_b) = \mathcal{T}(\vec{x}'; \vec{x}|\vec{c}_b) \otimes p_{MC}(\vec{x}|\vec{c}_b) \quad (2.3)$$

and applied to Monte Carlo distribution in a desired signal region \vec{c}_s as,

$$\hat{p}_{data}(\vec{x}'|\vec{c}_s) = \mathcal{T}(\vec{x}'; \vec{x}|\vec{c}_b) \otimes p_{MC}(\vec{x}|\vec{c}_s). \quad (2.4)$$

One of the assumptions of the data-driven techniques is that $\mathcal{T}(\vec{x}'; \vec{x}|\vec{c}_s) \approx \mathcal{T}(\vec{x}'; \vec{x}|\vec{c}_b)$, hence $\hat{f}_{data} \approx f_{data}$. Such assumptions can be checked to some degree by using simulated data. If there are enough CRs then the \mathcal{T} dependence on \vec{c} could be learned.

3 Neural Autoregressive Flows for Data-driven Shape Estimation

3.1 Neural Autoregressive Flows

Through deep generative methods, it is possible to approximate $p(\vec{x}; \vec{c})$ by training with data directly. A powerful way for deriving transformations is the normalizing flows method [16–18]. Through normalizing flows, feature variables are transformed through multidimensional invertible bijections. Such invertible bijections can be built using simple transformations. NF allow for probability density estimations and/or generation of variables that follow certain complicated distributions.

In this study, we adopt neural autoregressive flows, since it is simple, but allows for universal transformation [19]. In NAF, arbitrarily complicated transformations are created through a finite number of universal 1 dimensional transformations. This is made possible by the fact that multidimensional invertible bijection can be constructed in an autoregressive manner:

$$f(x_1, \dots, x_d) = f_1(x_1) f_2(x_2|x_1) \dots f_t(x_d|x_1, \dots, x_{d-1}), \quad (3.1)$$

where each f_j is invertible in x_j .

In NAF, the invertible transformations are built sequentially using a monotonic one dimensional function of x_i as,

$$\begin{aligned} y_1 &= \hat{f}_1(x_1; \theta_1(\vec{c}_0)) \\ y_2 &= \hat{f}_2(x_2; \theta_2(\vec{c}_0, x_1)) \\ &\dots \\ y_d &= \hat{f}_t(x_t; \theta_t(\vec{c}_0, x_1, \dots, x_{t-1})), \end{aligned} \tag{3.2}$$

where $t = 1, \dots, d$. The monotonic functions \hat{f}_t 's are neural networks where θ_t 's are the weights and biases of the network that depend on the previous inputs.

An invertible one dimensional function can be built with DNN's by using the sigmoidal function and its inverse, σ^{-1} , as:

$$\hat{f}_i(x_i; \theta_i) = \sigma^{-1} \left[\vec{W}^T(\theta_i) \cdot \sigma(\vec{a}_i(\theta_i)x + \vec{b}_i(\theta_i)) \right], \tag{3.3}$$

where $\vec{a}_i, \vec{b}_i, \vec{W}_i$ are h_i -dimensional vectors (h_i is a hyperparameter). The monotonicity is guaranteed if all elements of \vec{a}_i are positive. This is dubbed the deep sigmoidal flows (DSF) architecture. Despite its deceptive simplicity, DSF are shown to be universal approximators to any bijective transformations in real space [19].

3.2 NAF for shape estimation

We incorporate the DSF form of NAF for a restricted form of Eq. 2.2, with the effect of summation absorbed into p_{source} [23, 24].

$$\begin{aligned} p_{target}(\vec{x}'|\vec{c}') &= \int \mathcal{T}(\vec{x}'; \vec{x}|\vec{c}'; \vec{c}) p_{source}(\vec{x}|\vec{c}) d\vec{x} \\ &= \mathcal{T}(\vec{x}'|\vec{x}|\vec{c}'; \vec{c}) \otimes p_{source}(\vec{x}|\vec{c}) \end{aligned} \tag{3.4}$$

In order to apply the NAF method as normalizing flows, one of the probability densities, either $p_{source}(\vec{x})$ or $p_{target}(\vec{x}')$ for some \vec{c} must be known explicitly. However, in our case, neither of them is known analytically. Therefore, we use as the loss function to be minimized, the maximum-mean-discrepancy (MMD) which is a convex function suitable for comparing finite samples from two different multidimensional distributions [20].

The vectors $\vec{a}_i, \vec{b}_i, \vec{W}_i$ of Eq. 3.3 are output by multilayer perceptrons. And to satisfy the requirement of $a_{ij} > 0$, the activation function at the output used is the softplus function. And for \vec{W} , since $W_{ij} > 0$ and $\sum_j W_{ij} = 1$, softmax activation is used. For \vec{b} , no activation is used. The activation function for the hidden layers is $x\sigma(x)$, also known as the ‘‘swish’’ function. Compared to the often used ReLU function, this function is continuously differentiable everywhere and seems to provide the best performance in terms of the fidelity of the transformed distributions.

During training, minibatches are sampled from the source and target samples, picked randomly from the respective subsamples in the category \vec{c} and \vec{c}' . With the minibatch

¹ $\sigma(x) = 1/(1 + e^{-x})$
² $\log(1 + e^x)$

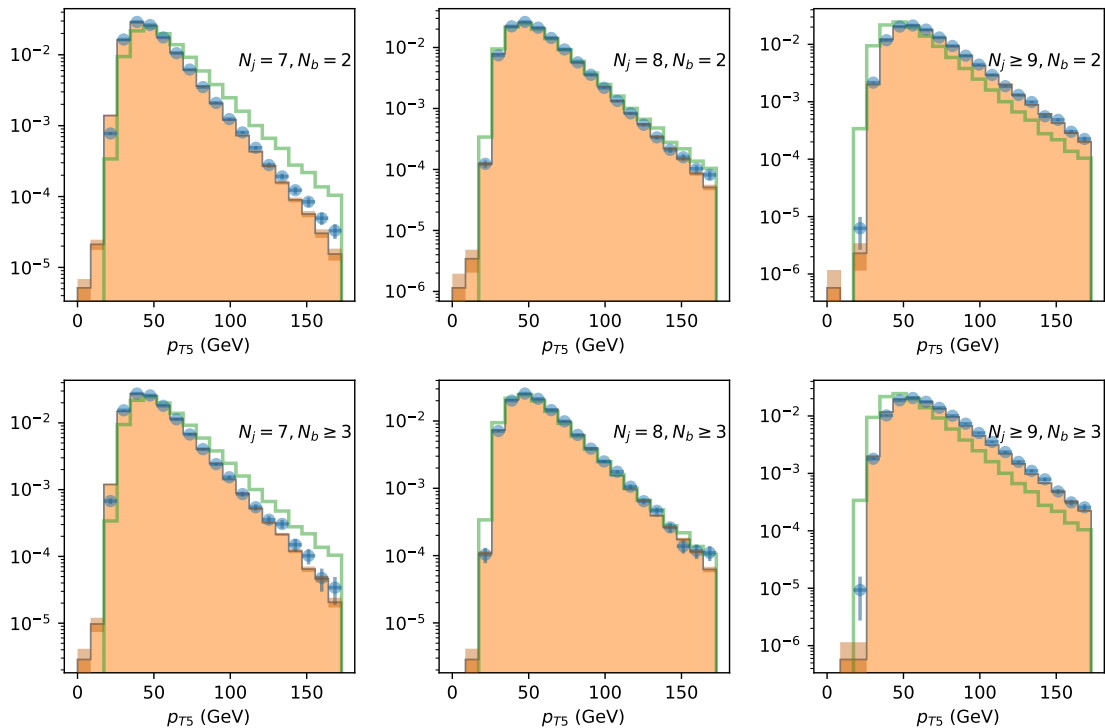


Figure 1. Distributions of the fifth leading jet p_T in different regions. Open histogram is the distribution for all the CR's combined. The NAF morphing is applied to match the original distribution (open histogram) to the real data in each region (points), and subsequent transformed distribution (solid histogram).

training, it is not possible to consider the absolute differences in the number of events. Therefore, with the current method, the shape prediction is possible but not the absolute normalization directly. However, it can be derived by adapting the method, since it is another differential distribution. Also, the extended ABCD method can be used for this purpose [22].

In the context of background estimation, the \vec{c} and \vec{c}' are used to label various control or signal regions. The CRs neighboring SR would have more similar distributions the closer they are to the SR. The distributions can be transformed to look like one another. Whether this can be done depends on how quickly the distribution $f(\vec{x}; \vec{c})$ changes depending on the condition \vec{c} . The premise of data-driven estimation is that background properties in the signal region can be inferred by interpolated or extrapolated from the information in the various CRs.

We could think of two ways to use these transformations for background predictions. One way is to apply transformation to a single source distribution as

$$\hat{p}_{data}(\vec{x}'; \vec{c}_i) = \mathcal{T}(\vec{x}', \vec{x}; \vec{c}_i, \vec{c}_0) \otimes p_{data}(\vec{x}; \vec{c}_0), \quad (3.5)$$

which we implement in Tensorflow 2.1 [23, 24]. Here, the NAF transformation learns how to transform a base distribution to each control region. For prediction in SR, condition

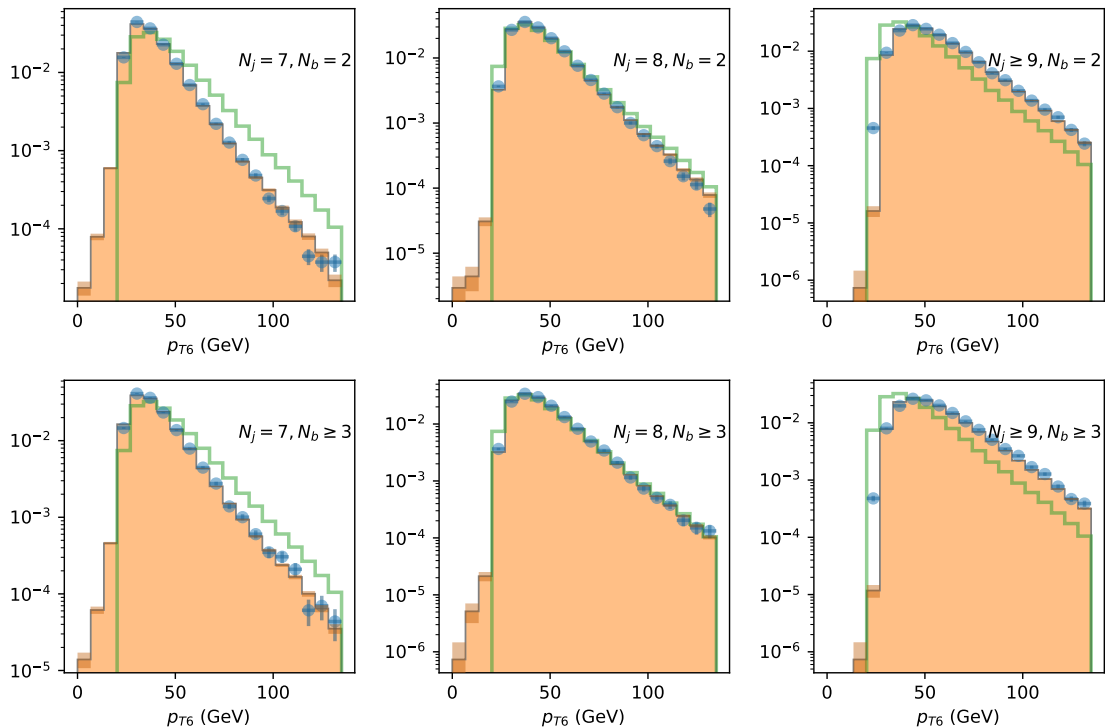


Figure 2. Distributions of the sixth leading jet p_T in different regions.

variable for SR is presented to the trained network. This could be a purely data-driven way of background estimation. The validity of the method and any systematic bias could be checked with simulation. In the next section, we demonstrate this method using simulated $t\bar{t} + \text{multijets}$ sample. Although, here \mathcal{T} is learned from the data, it could be learned from MC, and applied to data.

Secondly, the NAF transformation could be used to derive the shape corrections to the MC simulated sample from the CRs:

$$\hat{p}_{data}(\vec{x}'; \vec{c}_i) = \mathcal{T}(\vec{x}', \vec{x}; \vec{c}_i, \vec{c}_i) \otimes p_{MC}(\vec{x}; \vec{c}_i). \quad (3.6)$$

For this, the MC and data in the same CR are sampled and presented to the DNN for training. In this way, only the residual differences between simulation and data are learned. While in the first case, the changes going from CR to SR are to be extrapolated based solely on the CR without prior knowledge on anything about the SR. The physics difference among the various CR has to be learned by the transformation. In the second case, the important physics is already present in Monte Carlo, and by comparing with data in respective CR, only the residual differences to account for lack of detector understanding and some effects of higher-order contributions not present in MC would be learned. Therefore, in the second case, the transformation would mostly appear as small deviations away from 1. This would be a more appealing scenario for experimentalists.

The method can incorporate ABCD method, but is more general, since it can deal with multiple CRs or multiple control variables. And, we will label this method “ABCDnn” since

it uses DNN for ABCD type extrapolations. An added benefit of the ABCDnn method is that the transformation is interpretable since the transformation on each variable is a one dimensional function, which allows for further investigations.

The ABCDnn method would not be able to derive corrections for individual processes, but for the purpose of background estimation, it is less important. However, if desired, it would be still possible to incorporate different transformations to different samples by small modifications to the methods. For example, one could create a sample of MC with appropriate admixture of well understood backgrounds and another sample with larger uncertainties. During the training, we can choose minibatch and apply the transformation only to the less understood sample.

4 Application of ABCDnn to $t\bar{t} + multijets$

In this section, we apply Eq. 3.5 to $t\bar{t} + multijets$ simulated data. In our previous study, we found an analytic expression for an optimized method of extrapolation extending the ABCD method for the case of multiple CRs under some assumptions [22]. In the ABCD method, the two variables should be independent. With multiple CRs, non-linear dependence of the distributions on control variables and some effects of correlations among control variables can be reduced.

Through this case study, we would like to understand firstly, whether ABCDnn method can be used for extrapolations to SR estimate the distributions of various kinematic variables, and secondly, how it compares with the analytically derived extended ABCD method and whether it offers any advantages.

Data sample in this study was generated with MadGraph5 [25]. Process generated was $t\bar{t} + jj$ at leading order, where the W bosons from the top decays were forced to decay hadronically. This process was chosen as a proxy for backgrounds to many searches involving many jets in the final states. The generated sample was subsequently parton-showered and hadronized with Pythia 8 [26]. Finally, fast detector simulation and object reconstruction was done using Delphes 3 with the default settings [27]. The hadronic jet cone size used was $\Delta R = 0.4$, and the b-jets were identified through parameterized b-tagging efficiency and fake rates implemented in Delphes 3.

The control variables chosen were the number of hadronic jets (N_j) and the number of b-tagged jets in an event (N_b). For the baseline selection, we required $N_j \geq 7$ and $N_b \geq 2$. The signal region (SR) chosen was $N_j \geq 9$ and $N_b \geq 3$, and the remaining regions are CR's. We used the form 3.5 where we used the data sample in all the CR's together to form the source distribution.

The training was done by using minibatch scheme. We need two minibatches per training step, one from the target distribution and the other from the source distribution corresponding to \vec{c}_0 . The source minibatch is made by randomly sampling from data from all the CRs combined. And for the target minibatch, we first select the specific CR i.e. (N_j and N_b) by random sampling from all the CRs combined. Then, we randomly select events from that specific CR, so that samples within a minibatch have the same value of \vec{c} . Due to the discrete nature of the condition variables, they were “one-hot” encoded such that deep

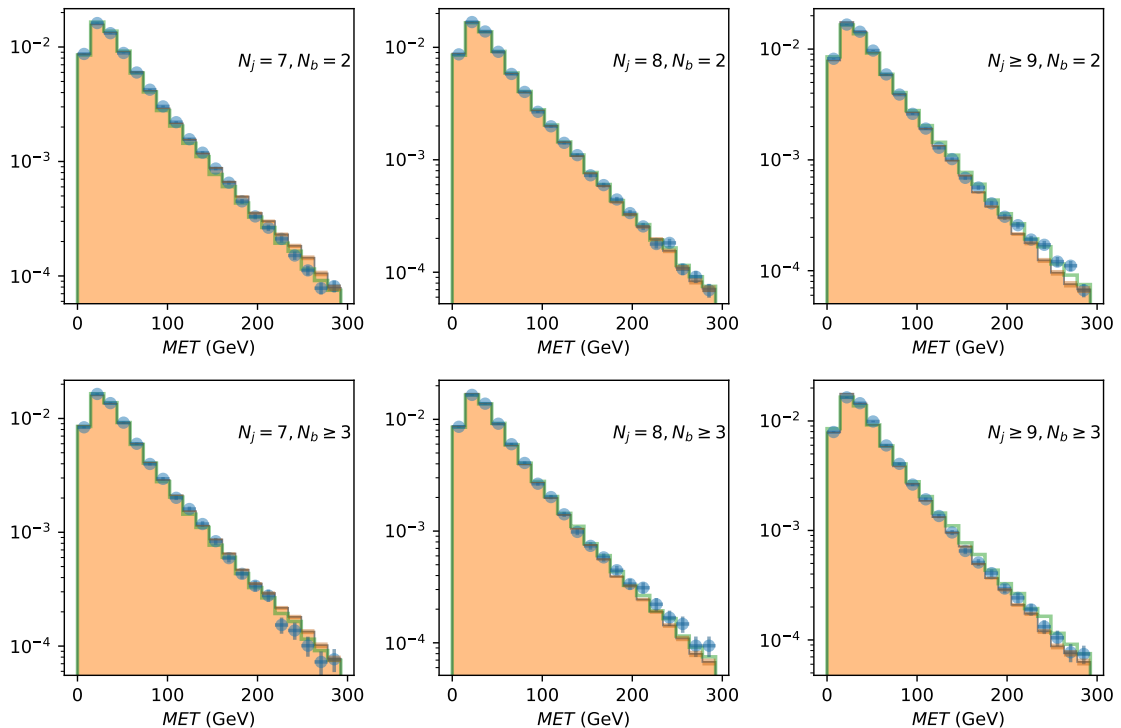


Figure 3. Distributions of missing E_T in different regions.

neural networks do not have difficulty in making use of this information. For more details on the setup, consult [23].

Figures 1 - 4 show some of the kinematic variables in $t\bar{t} + \text{multijets}$ sample. In each plot, the open histogram is the distribution of all CRs combined (the source), and they are identical across the six plots in each figure. The learned transformation is applied to the source data in CR which are shown as solid histograms. And the actual distributions (the target) are shown as solid points. The rightmost bottom plot is the SR. To make the prediction in SR, the condition variable for the SR is presented to the NAF transformation together with the source data for this purpose.

We can see that the transformations for each CR is properly learned. Also, for the SR, the shapes are well reproduced by the transformation. We emphasize that this transformation is not done on a variable by variable basis, but to all the feature variables simultaneously for a given event. Unless the correlations among variables are considered correctly it is extremely unlikely to obtain such agreement. We note that the transformed distribution has less fidelity in the region where there is a sharp cut off, such as near the p_T threshold of the hadronic jets. The hadronic jets were selected to have $p_T > 20\text{GeV}$, but the transformed p_T sometimes crosses this boundary, albeit at a very low rate. In practice, such events will be thrown away or assigned some systematic uncertainties for shape prediction.

By comparing the six plots in each figure, we can glimpse that the actual distributions, marked with solid points, show systematic trend as N_j or N_b changes, and this trend is what

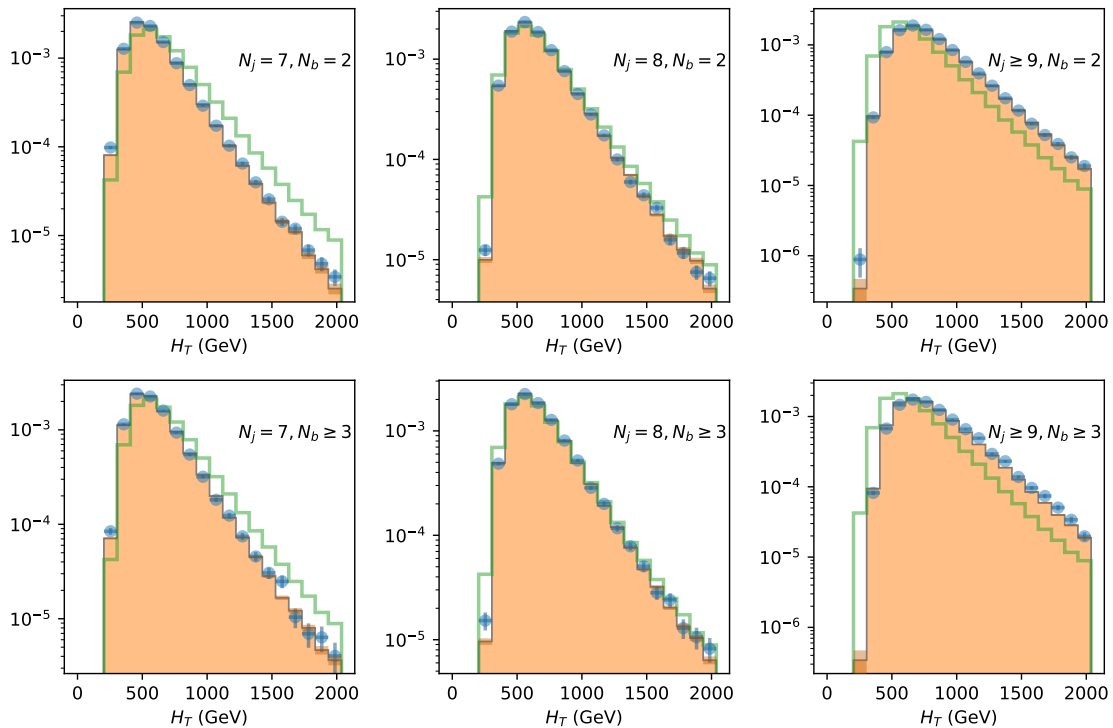


Figure 4. Distributions of H_T in different regions.

is learned by the NAF transformation when N_j and N_b is used as control variables. Taking Fig. 1 as an example, compared to the open histogram, the actual distributions become progressively harder as N_j increases. The spectra also become harder as N_b increases, by comparing the solid points in the top panes to those in the bottom panes, but to much lesser degree than N_j . If there is a component of the background that shows completely novel property in SR and which cannot be extrapolated from the CRs then this method would not be able to predict such novel feature. But this is expected.

In Figs. 5-6, we show distributions in the SR only and ratios to the true distributions, which illustrates the quality of the predictions with ABCDnn. We also compare them with the predictions made using the extended ABCD method [22]. The extended ABCD method makes use of distributions in multiple CR's and makes predictions in the SR by taking optimal (under some assumptions) products and divisions among the 1-D distributions in various CRs. By considering multiple CR's the extended ABCD method is able to take into consideration some non-linear dependence of the distributions on the control variables and weak correlation between the control variables, to some degree. The general tendencies of both predictions are similar and within statistical errors for the most part.

In each method, all the available statistics in CR is used for prediction in SR. However, the extended ABCD method can only be applied to one variable at a time and if some bin in one of the histogram has large statistical uncertainty then it will impact directly the final result, since products and divisions among the histograms in various CRs are used. While,

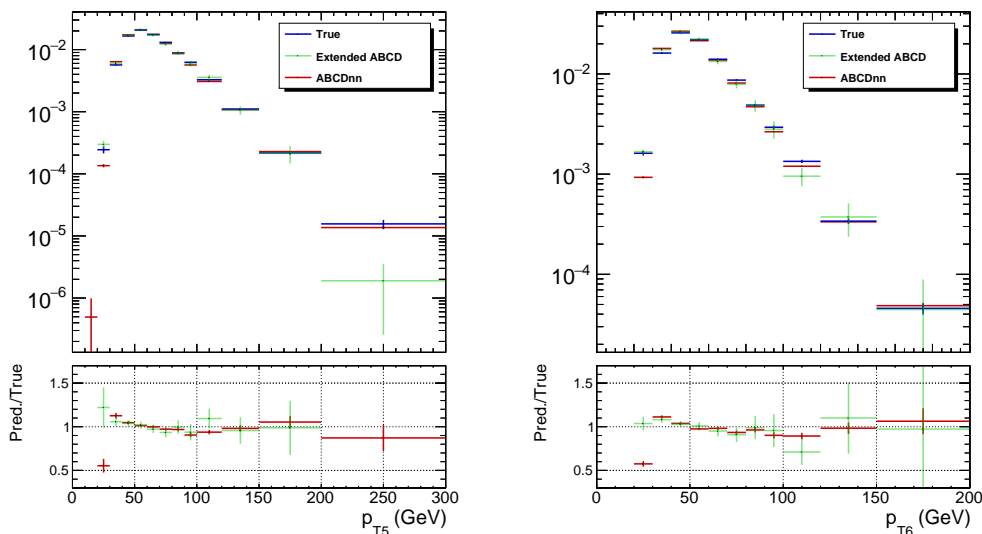


Figure 5. Normalized p_T distribution of the fifth and sixth leading jet in $N_{jet} \geq 9$ and $N_{bjet} \geq 3$ and predictions through the extended ABCD (green error bars) and ABCDnn (red error bars) methods

With the ABCDnn, multidimensional distribution is morphed in a non-linear manner by shifting values of the feature variables, and at the same time preserving correlation. We observe that the extended ABCD predictions have on average larger statistical uncertainties. Through this case study we demonstrated that the NAF transformation is able to learn transformations from CR and extrapolate it to SR. And interpreting the tendency compared to the extended ABCD method, we might interpret that the behavior is striving for optimal use of information available. Especially, ABCDnn makes the best use of the statistics available, while for extended ABCD method, the statistical uncertainty could not be taken into account when aiming for optimal use of data.

The ABCDnn method would allow systematic and automatic approach to background estimations, and it can be adapted to a more variety of use cases than what is considered here. This study was restricted to using the simulated data, in place of the real data, for the purpose of purely data-driven background shape estimation scenario. We can apply this method to a case where more than two control variables are used without any modifications, but this requires a dedicated study. And by modifying the method slightly, it is possible to implement Eq. 3.6, where only the corrections between the real data and the simulated data are learned, which would be appealing for experimentalists in deriving corrections to simulation and understanding their meaning. Although the background shape estimations was the primary focus of this study, with further modifications, it would be possible to estimate the relative event rates in each categories. (We note that while preparing the manuscript, an idea for using DNN for ABCD extrapolation appeared [28].)

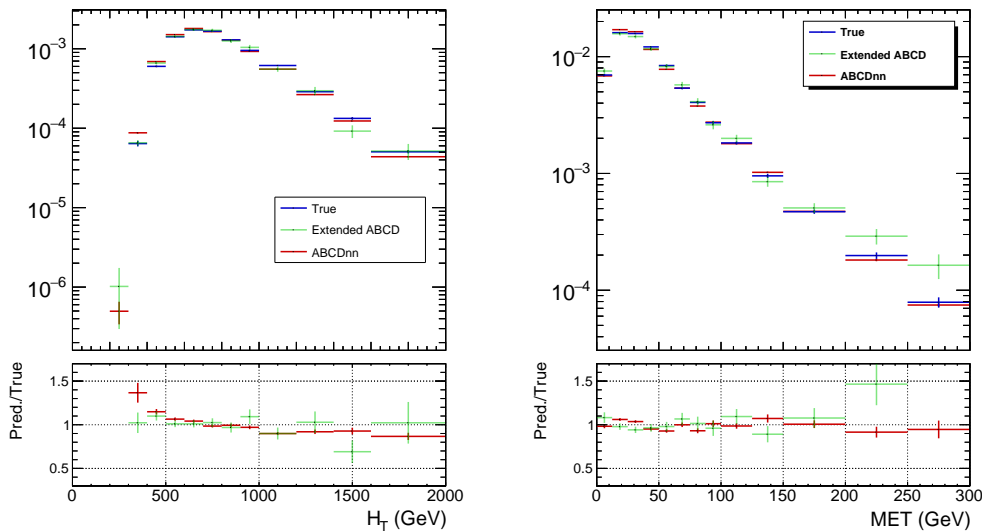


Figure 6. Normalized distribution of H_T and missing E_T of $t\bar{t} + \text{multijets}$ in SR ($N_{jet} \geq 9$ and $N_{bjet} \geq 3$) and predictions through the extended ABCD (green error bars) and ABCDnn (red error bars) methods.

5 Conclusions

We presented a novel general data-driven method using neural autoregressive flows (NAF) for obtaining background distributions, which we dubbed the ABCDnn method. Through the use of multiple control regions, the ABCDnn method learns the dependence of transformation on the control variables, and it is able to extrapolate/interpolate to region of interest that neighbors the control regions. Since the transformation is constructed out of a finite number of 1-D transformations, it is possible to understand or interpret it, unlike some DNN methods. Whereas existing data-driven estimation methods usually work on a single feature variable and it would be able to handle simultaneously many variables automatically while taking into account the correlations among feature variables, unlike existing methods. Moreover, the evidence from case study suggests that the prediction is close to optimal. This method can be used in many cases where the reliable predictions of backgrounds based solely on simulations is not available.

Acknowledgments

This work has been supported by Korean National Science Foundation through its mid-career grant.

References

- [1] G. Aad, *et al.* (ATLAS Collaboration), *A search for the dimuon decay of the Standard Model Higgs boson with the ATLAS detector*, arXiv:2007.07830.

- [2] CMS Collaboration, *Measurement of Higgs boson decay to a pair of muons in proton-proton collisions at $\sqrt{s} = 13$ TeV*, CMS Physics Analysis Summary HIG-19-006, <http://cms-results.web.cern.ch/cms-results/public-results/preliminary-results/HIG-19-006/index.html>.
- [3] A.M. Sirunyan, *et al.* (CMS Collaboration), *Observation of the production of three massive gauge bosons at $\sqrt{s} = 13$ TeV*, arXiv:2006.11191 (submitted to Phys. Rev. Lett.).
- [4] G. Bevilacqua, M. Worek, *On the ratio of $t\bar{t}b\bar{b}$ and $t\bar{t}jj$ cross sections at the CERN Large Hadron Collider*, J. High Energ. Phys. (2014) 2014: 135.
- [5] V. Khachatryan, *et al.* (CMS Collaboration), *Measurement of the cross section ratio $\sigma(t\bar{t}b\bar{b})/\sigma(t\bar{t}jj)$ in pp collisions at $\sqrt{s} = 8$ TeV*, Phys. Lett. B **746** (2015) 132.
- [6] A.M. Sirunyan, *et al.* (CMS Collaboration), *Measurement of the cross section for $t\bar{t}$ production with additional jets and b jets in pp collisions at $\sqrt{s} = 13$ TeV*, J. High Energ. Phys. (2020), 2020: 125.
- [7] J. J. Aubert, *et al.*, *Experimental Observation of a Heavy Particle J* , Phys. Rev. Lett. **33** (1974) 1404.
- [8] J. Augustin, *et al.*, *Discovery of a Narrow Resonance in e^+e^- Annihilation*, Phys. Rev. Lett. **33** (1974) 1406.
- [9] S. W. Herb, *et al.*, *Observation of a Dimuon Resonance at 9.5 GeV in 400-GeV Proton-Nucleus Collisions*, Phys. Rev. Lett. **39** (1977) 252.
- [10] F. Abe, *et al.* (CDF Collaboration). *Observation of Top Quark Production in $p\bar{p}$ Collisions with the Collider Detector at Fermilab*, Phys. Rev. Lett. **74** (1995) 2626.
- [11] S. Abachi, *et al.* (DØ Collaboration), *Observation of the Top Quark*, Phys. Rev. Lett. **74** (1995) 2632.
- [12] G. Aad, *et al.* (ATLAS Collaboration), *Observation of a new particle in the search for the Standard Model Higgs boson with the ATLAS detector at the LHC*, Phys. Lett. B **716** (2012) 1.
- [13] S. Chatrchyan *et al.* (CMS Collaboration), *Observation of a new boson at a mass of 125 GeV with the CMS experiment at the LHC*, Phys. Lett. B **716** (2012) 30.
- [14] Ian Goodfellow, *et al.*, *Generative Adversarial Nets*, Advances in Neural Information Processing Systems 27 (2014) 2672.
- [15] Mehdi Mirza and Simon Osindero, *Conditional Generative Adversarial Nets*, arXiv:1411.1784.
- [16] D. J. Rezende and S. Mohamed, *Variational Inference with Normalizing Flows*, arXiv:1505.05770.
- [17] L. Dinh, D. Krueger, and Y. Bengio, *NICE: Non-linear Independent Components Estimation*, arXiv:1410.8516.
- [18] I. Kobyzev, S. J.D. Prince and M. A. Brubaker, *Normalizing Flows: An Introduction and Review of Current Methods*, arXiv:1908.09257.
- [19] Chin-Wei Huang, David Krueger, Alexandre Lacoste, Aaron Courville, *Neural Autoregressive Flows*, arXiv:1804.00779.
- [20] Arthur Gretton, *et al.*, *A Kernel Two-Sample Test*, Journal of Machine Learning Research, 13(25):723, 2012.

- [21] O. Behnke *et al.*, *Data Analysis in High Energy Physics*, Wiley-VCH Verlag GmbH & Co. KGaA, (2013) pg. 334.
- [22] Suyong Choi and Hayoung Oh, *Improved Extrapolation Methods of Data-driven Background Estimation in High-Energy Physics*, arXiv:1906.10831.
- [23] <https://github.com/suyong-choi/ABCDnn>
- [24] https://www.tensorflow.org/versions/r2.1/api_docs/python/tf
- [25] J. Alwall, et al., *The automated computation of tree-level and next-to-leading order differential cross sections, and their matching to parton shower simulations*, JHEP 07 (2014) 079.
- [26] T. Sjöstrand, et al., *An Introduction to PYTHIA 8.2*, Comput. Phys. Commun 191 (2015) 159.
- [27] J. de Favereau, *et al.*, (Delphes3 Collaboration), *DELPHES 3, A modular framework for fast simulation of a generic collider experiment*, JHEP 02 (2014) 057.
- [28] Gregor Kasieczka, Benjamin Nachman, Matthew D. Schwartz, David Shih, *ABCDisCo: Automating the ABCD Method with Machine Learning*, arXiv:2007.14400.